Journal of Solid State Chemistry **158,** 49–54 (2001)
doi:10.1006/jssc.2000.9055, available online at http://www.idealibrary.com on IDEAL®

Chemical Deposition and Characterization of Cu_3Se_2 and CuSe Thin Films

Biljana Pejova[1] and Ivan Grozdanov

Institute of Chemistry, Faculty of Natural Sciences and Mathematics, Sts. Cyril and Methodius University, POB 162, Arhimedova 5, 91000 Skopje, Republic of Macedonia

Received August 2, 2000; in revised form December 4, 2000; accepted December 8, 2000;

A chemical deposition method for fabrication of Cu_3Se_2 and CuSe thin films is presented. The films' growth is based on the decomposition of selenosulfate in alkaline solution containing a copper(II) salt and a suitable complexing agent. The deposited materials were identified by X-ray diffraction. In addition, optical investigations were performed. The absorption onset in the optical spectra of the annealed Cu_3Se_2 films showed a slight red shift (compared to the as-deposited ones), indicating a very slight increase in the average crystal size. The optical (direct) band gap energy of Cu_3Se_2 thin films is 2.37 eV, while the CuSe thin films are characterized with two direct band gap energies of 2.0 and 2.8 eV. The average crystal size values, calculated on the basis of the recorded XRD patterns, are approximately 40 nm for both Cu_3Se_2 and CuSe thin films. © 2001 Academic Press

Key Words: **Cu_3Se_2 thin film; CuSe thin film; chemical bath deposition method; semiconductors; band gap energy.**

1. INTRODUCTION

Metal chalcogenide compounds, having a semiconductor nature, are of considerable technical interest in the field of electronics and electro-optical devices. Intensive research has been performed in the past to study the fabrication and characterization of these compounds in the form of thin films. Thus, the interest for copper selenides semiconducting thin films is motivated by their application in solar cell technology (1–3). In the literature, a number of methods for preparation of Cu_xSe thin films (where $x = 1$, 2 or between 1 and 2) have been reported (4–11). However, thin films of Cu_3Se_2 are much less exploited materials. While this work was near completion, a paper dealing with chemical bath deposition of Cu_3Se_2 and CuSe films appeared (12).

In our laboratory we continue to develop various chemical deposition methods for production and characterization of semiconducting metal chalcogenide thin films (13–19). Thus, the chemical deposition methodology for metal selenides (mercury(II) selenide (13), silver selenide (14), and lead(II) selenide (15)) and mercury sulfide (16) is based on the decomposition of selenosulfate as a selenide and thiosulfate as a sulfide ion precursors in an alkaline medium correspondingly and slow dissociation of complexed metal ions. The fabrication of metal oxides thin films (Fe_2O_3 (17), NiO (18), and CoO (19)) is based on thermal treatment of an aqueous solution that contains metal(2 +) ions and urea as hydroxide ions precursors and subsequent thermal conversion of the obtained hydroxide thin films to oxides.

In this paper, a chemical deposition method for preparation of Cu_3Se_2 and CuSe thin films on flexible substrates is reported. The structure and composition of the obtained films are discussed on the basis of X-ray diffraction data. Some optical characteristics of the films are also reported. The mechanical properties of the used substrates allow various possibilities for application of the obtained thin films.

2. EXPERIMENTAL PROCEDURE

2.1. *Preparation of the Substrates*

Thin films of Cu_3Se_2 and CuSe were deposited onto transparent, flexible polyester substrates with dimensions of ca. standard microscope glass. Prior to deposition, the substrates were treated with fresh 0.03% solution of $SnCl_2$ for about 15 min. Then, they were rinsed with deionized water and dried at room temperature before use. The treatment of the substrates with the solution of $SnCl_2$ improves the wetting of the surface of the substrate and improves the film adhesion. Most probably, this could be attributed to the formation of an ultra-thin film of tin(II) hydroxide chloride on the surface of the substrate as a result of the hydrolysis of tin(II) chloride (20).

2.2. *Thin Film Deposition*

Formation of Cu_3Se_2 and CuSe thin films is based on chemical decomposition in alkaline media. The proposed

---

[1] To whom correspondence should be addressed. Fax: + 389-91-226-865. E-mail: biljana@iunona.pmf.ukim.edu.mk.

0022-4596/01 $35.00

methodology used trisodium citrate as a complexing agent and aqueous solution of selenosulfate as a selenide anion precursor. For thin film depositions, the following stock aqueous solutions were prepared: 0.1 mol dm^{-3} $CuSO_4$, 0.1 mol dm^{-3} trisodium citrate, 1 mol dm^{-3} Na_2SeSO_3, and 1 mol dm^{-3} NaOH. The solution of sodium selenosulfate was synthesized by dissolving elemental Se in a sodium sulfite solution and heating the obtained mixture for about 1 h at approximately 90°C. Sulfite ions, present in excess, have an important role in stabilizing the selenosulfate solution due to their reducing properties. The decomposition of selenosulfate solution and formation of red, colloidal selenium is prevented by excess of sodium sulfite. Hence, sulfite cannot only function as an oxidizing inhibitor, itself forming sulfate, but can also react with the selenium that may be initially present to form selenosulfate and thus preventing the deposition of red, colloidal selenium (21).

2.2.1. Cu_3Se_2 thin film deposition. For Cu_3Se_2 film growth, the deposition solution was prepared by mixing equal volumes (6 cm^3) of the stock solutions of copper(II) sulfate and sodium citrate and adding 3 cm^3 solution of selenosulfate and deionized water to make a total volume of 100 cm^3. Upon the addition of the sodium citrate to copper(II) sulfate solution, a clear blue solution is created as a result of the formation of a complex between Cu^{2+} and Cit^{3-}. The pH of the deposition solution was 9.

Previously treated substrates were vertically introduced in the deposition solution. The film deposition was carried out at approximately 60°C. Upon heating for approximately 15 min, the deposition process starts and the color of the solution turns to dark brown. After the deposition process, the obtained thin films were rinsed with distilled water and dried in air. It takes several hours to deposit Cu_3Se_2 films (depending on the required thickness). The terminal thickness of deposited films, from one bath, is about 100 nm.

2.2.2. CuSe thin film deposition. For copper(II) selenide thin film growth, the deposition bath is composed of 4 cm^3 0.1 mol dm^{-3} solution of copper sulfate, 4 cm^3 0.1 mol dm^{-3} solution of sodium citrate, 3 cm^3 solution of selenosulfate, 1 cm^3 1 mol dm^{-3} solution of sodium hydroxide, and distilled water to a total volume of 100 cm^3. The pH of the deposition solution was 12.

The treated substrates were vertically introduced in the deposition solutions. The film deposition was carried out at approximately 60°C. After the deposition process, the obtained thin films were rinsed with distilled water and dried in air. The terminal thickness of deposited CuSe, from one bath, is about 200 nm.

2.3. Characterization of the Obtained Thin Films

2.3.1. X-ray diffraction (XRD). X-ray diffraction patterns of the fabricated thin films, deposited on transparent polyester substrates, were recorded on a Philips PW 1710 diffractometer, using Cu$K\alpha$ radiation. The technique of XRD allowed the characterization of the crystal composition, structure, and the calculation of the average crystal size using the Debye–Scherrer relationship.

2.3.2. Optical characterization. Optical spectra of obtained thin films were recorded using a Varian UV-Vis-NIR spectrophotometer with a polyester substrate as a reference.

2.3.3. Light scattering experiments. Light scattering experiments were carried out on the deposition solution. Shining short wavelength laser light (400 nm) through the solution allowed the presence or absence of a colloid in the solution to be seen, by visual observation, due to scattering of the laser beam by colloidal particles.

2.3.4. Film thickness determination. The thicknesses of the films were determined by the gravimetric method using the relation $d = m/(\rho \cdot S)$ where m and S are the mass and the surface area of equally covered parts of the substrate, respectively, while ρ is the density of the bulk material.

3. RESULTS AND DISCUSSION

3.1. Chemical Considerations

Chemical deposition of CuSe and Cu_3Se_2 is based on decomposition of selenosulfate in alkaline solution containing a copper(II) salt and a suitable complexing agent that allows us to control the Cu^{2+} ions concentration. The precipitation process can take place either in the bulk of the solution (homogeneous process) or at the substrate surface (heterogeneous process), the second leading to film formation (22). The film solution growth can occur by two distinct routes: ion-by-ion mechanism and cluster or colloidal mechanism (23).

In an alkaline medium, the selenosulfate anion hydrolyzes to hydrogenselenide and selenide ions:

$$SeSO_3^{2-} + OH^- = HSe^- + SO_4^{2-} \tag{1}$$

$$HSe^- + OH^- = H_2O + Se^{2-}. \tag{2}$$

According to the ion-by-ion mechanism (i.e., growth by successive anion and cation adsorption on the growing crystal), the formation of copper(II) selenide can be written as follows:

$$[Cu(Cit)]^- = Cu^{2+} + Cit^{3-} \tag{3}$$

$$Cu^{2+} + Se^{2-} = CuSe. \tag{4}$$

Selenide anions are generated by the slow alkaline hydrolysis of selenosulfate, while Cu^{2+} cations are released by dissociation of the complexed ions. It is well known that, in an alkaline medium, copper(2 +) ions in the presence of organic compounds that contain hydroxyl groups (for example, citric acid and tartaric acid) do not precipitate copper(II) hydroxide, but form a blue-colored complex. The deposition of CuSe occurs when the concentrations of copper(2 +) and selenide(2 −) ions are such as to exceed the solubility product of the CuSe. In the case of Cu_3Se_2 bath deposition, the sulfite anion, having reducing properties, can reduce Cu^{2+} into Cu^{+} ions. The deposition of Cu_3Se_2 can occur when the ion concentration product of Cu^{2+}, Cu^{+}, and Se^{2-} exceeds the solubility product of the Cu_3Se_2.

$$2Cu^{2+} + SO_3^{2-} + 2OH^{-} = 2Cu^{+} + SO_4^{2-} + H_2O \qquad [5]$$

$$Cu^{2+} + 2Cu^{+} + 2Se^{2-} = Cu_3Se_2. \qquad [6]$$

According to the cluster mechanism, film growth is based on absorption and coagulation of colloidal particles. The colloidal particles are, probably, metal chalcogenide or metal hydroxide species (22, 23). Chalcogenide (in our case selenide) anions, generated by a slow hydrolysis of selenosulfate, could replace hydroxyl groups and convert metal hydroxide to metal chalcogenide. This ability of the selenide anions is due to the lower solubility product of both CuSe and Cu_3Se_2 compared to that of copper hydroxide.

It is known that, if film growth occurs by an ion-by-ion mechanism, no bulk precipitation should be observed in the deposition solution (22). On the other hand, if the film formation process occurs by a cluster mechanism, bulk clusters are visible in the deposition solution. It has been shown that even if no visible colloidal species are formed in the solution, the cluster mechanism can still occur by absorption of colloidal particles (not visible to the naked eye) on the substrate surface and coagulation (23).

In our case, light scattering experiment showed that the cluster mechanism is dominant in the growth processes for both film types. For the largest part of deposition processes, bulk precipitation, accompanied by scattering of the laser beam, is observed. However, at the end of the depositions, bulk precipitation and light scattering reduce. This may be due to the ion-by-ion growth. It can be concluded that both mechanisms may interact, leading to the film formation at the end of the deposition process.

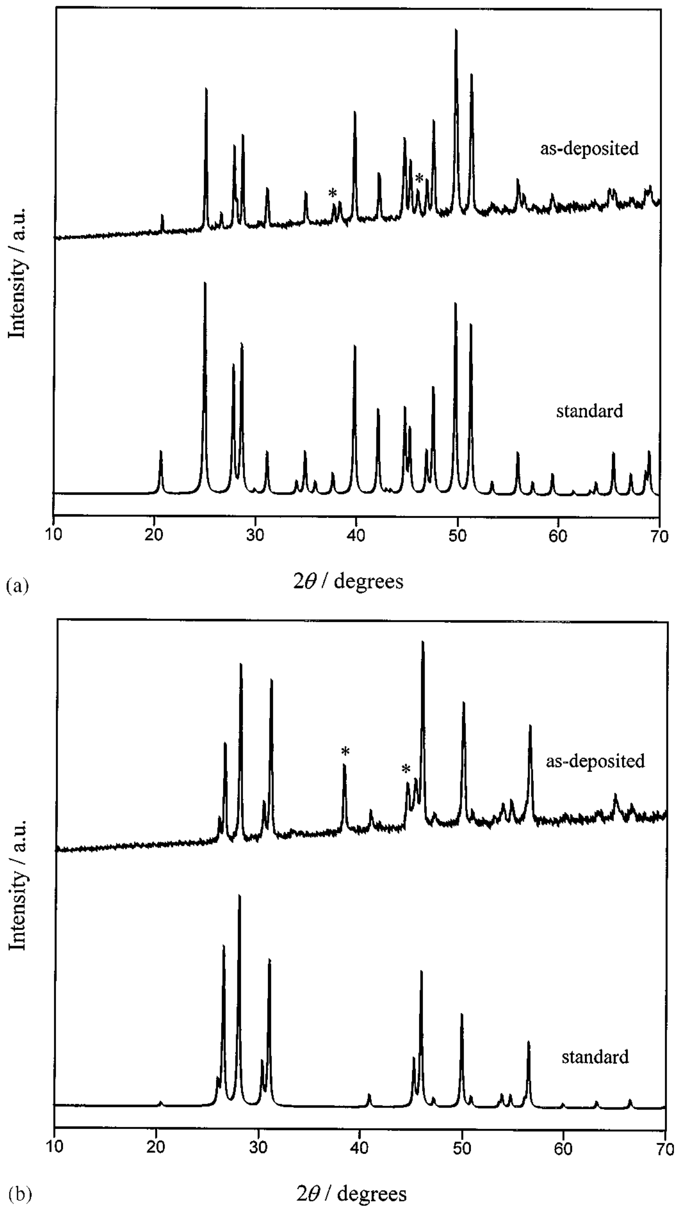

FIG. 1. (a) XRD patterns of as-deposited Cu_3Se_2 material and standard (the peaks marked with an asterisk (appearing at 2θ values of 38.35° and 44.59°) are from the Al sample carrier—see for example, Ref. (28)). (b) XRD patterns of as-deposited CuSe material and standard (the peaks marked with an asterisk (appearing at 2θ values of 38.35° and 44.59°) are from the Al sample carrier—see for example, Ref. (28)).

3.2. X-ray Investigations

3.2.1. X-ray investigations of Cu_3Se_2. Identification of the obtained thin films was carried out using the X-ray diffraction method. The recorded XRD pattern of as-deposited material is presented in Fig. 1a. All peaks of the diffractogram were found to be characteristic of polycrystalline Cu_3Se_2, modification known as umangite, with a tetragonal structure and crystal parameters $a = 6.402$ Å and $c = 4.276$ Å (24). According to the X-ray study, the obtained films are pure Cu_3Se_2 (i.e., the impurities, if present, are below the detection limit of the X-ray diffractometer). They are characterized with random orientation and show no sign of texturing. The recorded XRD spectrum of annealed material (at *ca.* 120°C in air) did not show significant improvement in crystallinity upon annealing.

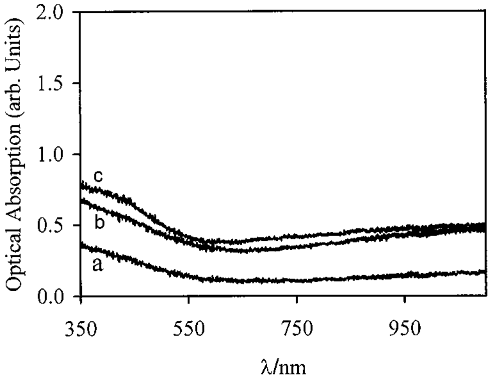

FIG. 2. Absorption spectra of as-deposited Cu_3Se_2 thin films with thicknesses of 22 (a), 65 (b), and 94 nm (c).

The average crystal size was estimated using the well-known Debye–Scherrer relationship (25):

$$d = \frac{0.9 \cdot \lambda}{\beta \cdot \cos\theta} \qquad [7]$$

were θ is the Bragg angle, λ is the X-ray wavelength, and is the full width at half-maximum. It was found that the average crystal size is 42 nm.

3.2.2. X-ray investigations of CuSe. The recorded XRD pattern of as-deposited copper(II) selenide is presented in Fig. 1b. As can be seen, the comparison with the simulated XRD pattern (26) confirms that the obtained material is nontextured pure copper(II) selenide, modification known as klockmannite with hexagonal structure and crystal parameters $a = 3.939$ Å and $c = 17.255$ Å. Using the previously mentioned Debye–Scherrer relation, the average crystal size

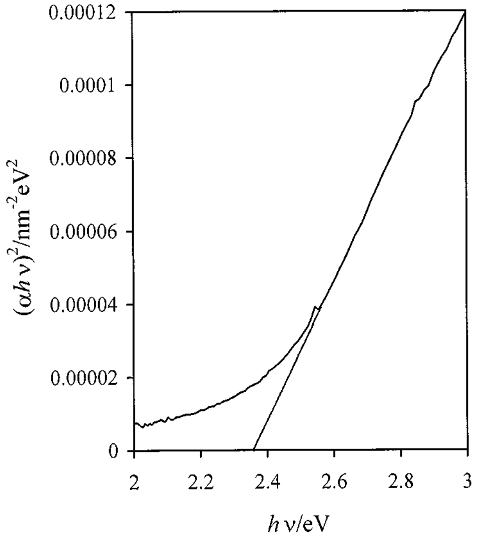

FIG. 4. The dependence of $(\alpha h\nu)^2$ on $h\nu$ for as-deposited Cu_3Se_2 film.

was found to be about 42 nm. In this case also the annealing process practically does not improve the film crystallinity.

3.3. Optical Measurements

3.3.1. Optical measurements of Cu_3Se_2 thin films. For optical characterization, UV–Vis–NIR spectra of as-deposited and annealed Cu_3Se_2 thin films were recorded using polyester substrate as a reference. The absorption spectra of as-deposited thin films of Cu_3Se_2 with different thicknesses (22, 65, and 94 nm) are presented in Fig. 2. It is seen that the as-deposited thin films are highly transparent in the Vis–NIR spectral region. At about 550 nm an absorption onset is evident. In Fig. 3, optical transmittance spectra of both unannealed and annealed Cu_3Se_2 films with equal thicknesses are shown. A slight red shift of the absorption onset is observable upon annealing, indicating a rather

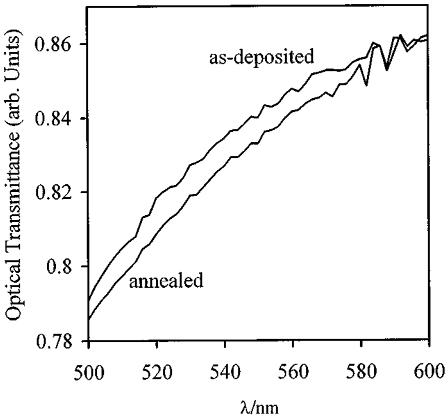

FIG. 3. Optical transmittance spectra of both Cu_3Se_2 unannealed (a) and annealed (b) films.

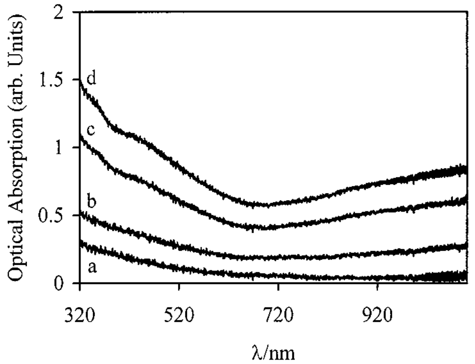

FIG. 5. Absorption spectra of as-deposited CuSe thin films with thicknesses 45 (a), 70 (b), 118 (c), and 168 nm (d).

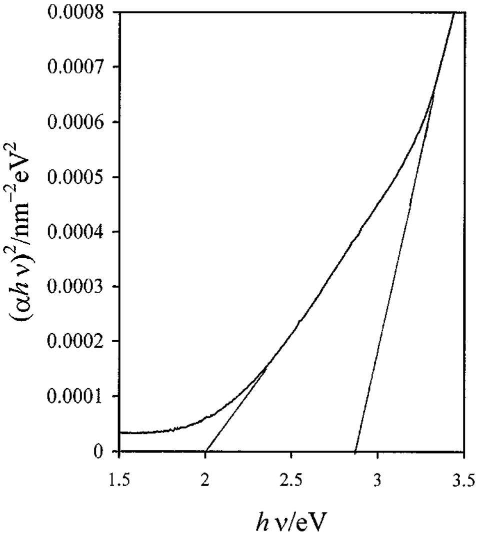

FIG. 6. The dependence of $(\alpha h\nu)^2$ on $h\nu$ for as-deposited CuSe film.

small increase in the average crystal size with heat treatment. The red shift observed in the absorption onset upon annealing may be due to an increase in grain size (27), and in principle it would be expected to reflect in the decrease of band gap energy as well. However, in the present case the effect is very small and no measurable changes in the last quantity have been observed. Also, no measurable changes in the full widths at half-maximum intensity of XRD peaks for the as-deposited and annealed films could be detected.

The optical band gap (E_g) for as-deposited and annealed films was calculated on the basis of the optical absorption spectra, using the well-known relation

$$\alpha h\nu = A(h\nu - E_g)^n, \qquad [8]$$

where A is constant, $h\nu$ is the photon energy, and α is the absorption coefficient, while n depends on the nature of the transition. For direct transitions $n = \frac{1}{2}$ or $\frac{3}{2}$, while for indirect ones $n = 2$ or 3, depending on whether they are allowed or forbidden, respectively. The best fit of the experimental curve to a band gap semiconductor absorption function of both the as-deposited and annealed pattern was obtained for $n = \frac{1}{2}$. The calculated value of the direct energy band gap is 2.37 eV for both as-deposited and annealed Cu_3Se_2 thin films. In Fig. 4, the dependence of $(\alpha h\nu)^2$ versus $h\nu$ is presented for as-deposited thin film of Cu_3Se_2. This value is somewhat lower than the recently published one (12), which may be due to the size quantization effect as well as to differences due to various deposition mechanisms and conditions involved. (It has been well recognized that the value of the band gap energy is affected by the deposition technique and deposition conditions.)

3.3.2. Optical measurements of CuSe thin films. The recorded optical spectra for as-deposited thin films of copper(II) selenide with different thicknesses (45, 70, 118, and 168 nm) in the UV–Vis–NIR spectral region are presented in Fig. 5. The thin films are transparent in the spectral region from approximately 650 to 1100 nm. Upon annealing, the shift of the absorption onset is not observed, indicating no changes in the average crystal size and in the band gap energy of the annealed thin films. Using the recorded optical spectra and the relation [8], optical band gap energies of both unannealed and annealed CuSe thin films were calculated. Copper(II) selenide thin films, as-deposited and annealed, are direct semiconductors; i.e., the best fit of the experimental curve to a band gap semiconductor absorption function was obtained for $n = \frac{1}{2}$. The extrapolation of the linear part of the curves gave two values for direct band gap energy of 2.0 and 2.8 eV for both unannealed and annealed films. The first value of the optical band gap agrees with the previously reported one for copper(II) selenide thin films by A. Mondal and P. Pramanik (4). On Fig. 6 the dependence of $(\alpha h\nu)^2$ versus $h\nu$ for as-deposited copper(II) selenide thin films is presented.

REFERENCES

1. J. J. Loferski, *J. Appl. Phys.* **27,** 777–784 (1956).
2. H. Okimura, T. Matsumae, and R. Makabe, *Thin Solid Films* **71,** 53–59 (1980).
3. W. S. Chen, J. M. Stewart, and R. A. Mickelsen, *Appl. Phys. Lett.* **46,** 1095–1097 (1985).
4. A. Mondal and P. Pramanik, *J. Solid State Chem.* **47,** 81–83 (1983).
5. T. L. Chu, S. S. Chu, S. C. Lin, and J. Yue, *J. Electrochem. Soc.* **131,** 2182–2185 (1984).
6. G. K. Padam, *Thin Solid Films* **150,** L89–L92 (1987).
7. S. K. Haram, K. S. V. Santhanam, M. Neumann-Spallart, and C. Lévy-Clément, *Mater. Res. Bull.* **27,** 1185–1191 (1992).
8. S. Massaccesi, S. Sanchez, and J. Vedel, *J. Electrochem. Soc.* **140,** 2540–2546 (1993).
9. L. Thouin, S. Rouquette-Sanchez, and J. Vedel, *Electrochim. Acta* **38,** 2387–2394 (1993).
10. I. Grazdanov, *Synthetic Met.* **63,** 213–216 (1994).
11. C. Lévy-Clément, M. Neumann-Spallart, S. K. Haram, and K. S. V. Santhanam, *Thin Solid Films* **302,** 12–16 (1997).
12. M. Lakshmi, K. Bindu, S. Bini, K. P. Vijayakumar, C. S. Kartha, T. Abe, and Y. Kashiwaba, *Thin Solid Films* **370,** 89–95 (2000).
13. B. Pejova, M. Najdoski, I. Grozdanov, and S. K. Dey, *J. Mater. Chem.* **9,** 2889–2892 (1999).
14. B. Pejova, M. Najdoski, I. Grozdanov, and S. K. Dey, *Mater. Lett.* **45,** 269–273 (2000).
15. I. Grozdanov, M. Najdoski, and S. K. Dey, *Mater. Lett.* **38,** 28–32 (1999).
16. M. Najdoski, I. Grozdanov, S. K. Dey, and B. Siracevska, *J. Mater. Chem.* **8,** 2213–2215 (1998).
17. B. Pejova, M. Najdoski, I. Grozdanov, and A. Isahi, *J. Mater. Sci.: Mater. Electron.* **11,** 405–409 (2000).
18. B. Pejova, T. Kocareva, M. Najdoski, and I. Grozdanov, *Appl. Surf. Sci.* **165,** 271–278 (2000).
19. B. Pejova, A. Isahi, M. Najdoski, and I. Grozdanov, *Mater. Res. Bull.*, in press.

20. I. Filipovič and S. Lipanovič, "General and Inorganic Chemistry," Part II, p. 845. Skolska Knjiga, Zagreb, 1991.
21. R. A. Zingaro and D. O. Skovlin, *J. Electrochem. Soc.* **111,** 42–47 (1964).
22. M. Froment and D. Lincot, *Electrochem. Acta* **40,** 1293–1303 (1995).
23. S. Gorer, A. Albu-Yaron, and G. Hodes, *Chem. Mater.* **7,** 1243–1256 (1995).
24. JCPDS – International Centre for Diffraction Data set no. 08-0279.
25. M. T. Welller, "Inorganic Materials Chemistry," p. 25, Oxford Science, Oxford, 1994.
26. JCPDS – International Centre for Diffraction Data set no. 34-0171.
27. S. Gorer and G. Hodes, *J. Phys. Chem.* **98,** 5338–5346 (1994).
28. A. Šurca, B. Orel, B. Pihlar, and P. Bukovec, *J. Electroanal. Chem.* **408,** 83–100 (1996).